Analysis of Switched Inductor Three-level DC/DC Converter

E. Salary, M. R. Banaei, A. Ajami

Department of Electrical Engineering, Azarbaijan Shahid Madani University, Tabriz, Iran

Abstract- A non-isolated DC/DC converter with high transfer gain is proposed in this paper. The presented converter consists of the switched inductor and three-level converters. The DC/DC power converter is three-level boost converter to convert the output voltage of the DC source into two voltage sources. The main advantages of DC/DC converter are using low voltage semiconductors and high gain voltage. The steady-state operation of the suggested converter is analyzed. A prototype is developed and tested to verify the performance of the proposed converter. To sum up, the MATLAB simulation results and the experimental results have transparently approved high efficiency of proposed converter as well as its feasibility.

Keyword: renewable energy sources, PV-Battery system, non-isolated DC/DC converter, high gain DC/DC converter.

1. INTRODUCTION

Renewable energy sources such as photovoltaic (PV) arrays, wind turbine, gas micro turbine and fuel cells have been increasing at a fast step in distributed power systems. The obvious distinctive of these sources is low voltage supply with wide range voltage drop and in some cases generated energy depends on weather condition [1-4]. With regard to this characteristic, distributed power systems, have to employ a high step-up DC/DC converter [4]. In conventional DC/DC boost converter, in practical cases, the duty ratio cannot tends to be the extreme value unity [4-6]. When the conventional DC/DC boost converter operates under the high duty ratio, the high-frequency EMI issue and efficiency are unfavorable [8]. Typical solutions include the use of high gain DC/DC boost converter to adjust the voltage gain. The use of high-frequency transformers is one solution to obtain desired voltage gain. This may result in an increased size and weight when compared with non-isolated DC/DC converters. For example, the main drawbacks in full-bridge DC/DC converter with high-frequency transformers are complexity and the need for four sets of active switches. Cascading one or more conventional

DC/DC converters is other way to obtain high step-up power conversions. Switched-capacitor/inductor network provides another solution to achieve high step-up voltage gain. Several converters exist to achieve DC/DC voltage conversion. Each of these converters has its specific benefits and disadvantages, depending on a number of operating conditions and specifications [9-19]. The interleaved double dual boost converters are one type of high gain DC/DC converter [9-12]. The main drawback of these topologies are complex control and using a large number of active switches. In [12] a new topology is proposed with the objective of creating a higher voltage gain in comparison with the classical boost converter, i.e., the interleaved double dual boost converter. The presented topology in [13], uses two intermediary capacitors to double the output voltage when compared to the conventional boost converter. The new circuits, also named diode-assisted DC/DC converters [14], enhance the voltage boost/buck capability and avoid the extreme duty ratio. Some DC/DC buck–boost converters are recently presented by using the KY converters. KY converters are also used to construct high step-up converters like in [15]. In [16], a new buck–boost converter is proposed. The voltage gain of the proposed converter in step-up mode is higher than the basic non-isolated buck–boost converters. In [17] a two stage converter is proposed for AC-module photovoltaic (PV) system. The proposed system consists of a high-voltage gain switched inductor boost inverter. The switched inductor boost converter (SIBC) has one switch operates like a continuous conduction mode. The

SIBC gives high gain by using switched inductor circuit. A new power conversion system is explored in [16] aiming wind turbines. The proposed configuration uses a DC/DC four-level boost converter as the intermediate stage. A photovoltaic (PV) system using multilevel boost converter (MBC) and line commutated inverter (LCI), operating in both grid-connected mode and stand-alone mode has been analyzed in [17]. The DC/DC converter in [17] has one active switch but it uses a large number of diode and capacitors.

The DC/DC converter can be used in multilevel inverters [21-23].

In this paper, high gain DC/DC converter is proposed which is suitable for energy conversion applications. The proposed converter topology is the combination of three-level converter and high gain switched inductor boost converter. The gain of voltage can be increases by adding switched inductor circuits. Analysis, simulation and experimental set-up are introduced to verify the proposed system performances.

2. DC/DC CONVERTER

In a classic DC/DC boost converter, the voltage stresses on switch and diode, which are equal to the output voltage, are high. In the three-level step-up DC/DC converter semiconductor device voltage rating is only half of the output voltage [10-12]. In these converter special modulation technique, offers lower input current ripple, too. The boost and voltage-doublers techniques are integrated in the three-level boost converter to achieve higher step-up voltage gain compared to conventional boost converter. The peak inverse voltage of switches and diodes is half of output voltage. In this paper, a new DC/DC converter based on three-level DC/DC converter is analyzed. The proposed converter gives higher gain than conventional boost and three-level boost converters. The circuit configuration of the presented converter is shown in Fig. 1.

As shown in Fig. 1, the proposed converter consists of voltage-doublers circuit and switched inductor circuits. The switched inductor composed of two diodes and two inductors.
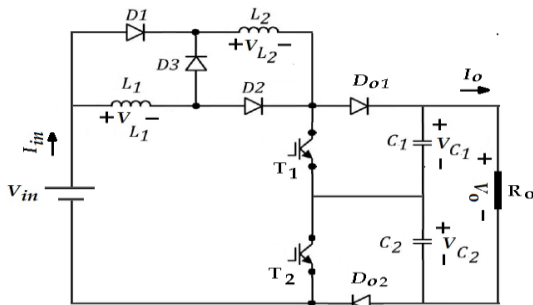
Fig. 1. Configuration of the proposed converter.

2.1. Operating principles of the proposed converter

In order to simplify the circuit analysis of the converter, all components are assumed ideal and the voltage of output capacitors of DC/DC converter is equal. Capacitors C_1, C_2 and inductor are large enough. Thus, voltage of capacitors and current of inductors is considered as constant in one switching period. It is assumed that converter has one resistive load, too.

The voltage of output capacitors is equal.

$$V_{C1} = V_{C2} = \frac{V_O}{2} \tag{1}$$

The output voltage is equal to sum of voltage of output capacitors.

$$V_O = V_{C1} + V_{C2} \tag{2}$$

Figure 2 shows the topological stages of the proposed converter. The operating modes are described as follows.

Mode 1: Fig. 2(a) shows mode 1 equivalent circuits. During this mode T_1 and T_2 are turned on. The DC-source energy is transferred to L_1 and L_2. In this mode inductors are series.

The voltage of inductors has positive value. In this mode D_1, D_2 are turned on and D_3, D_{o1} and D_{o2} are turned off. Energy of output capacitors is given to load and capacitors put on in discharge mode.

$$V_{L1} = V_{in} \tag{3}$$

$$V_{L2} = V_{in} \tag{4}$$

Duration of mode 1 is equal as:

$$t_1 = D.T = \frac{D}{f} \tag{5}$$

D, T and f are the duty cycle switching period and switching frequency respectively.

Mode 2: T_1 is turned on and T_2 is turned off. In this mode D_3, D_{o2} are turned on and D_1, D_2 and D_{o1} are turned off. The voltage of inductors has negative value and energy is pumped to C_2 while energy of C_1 is given to load. The currents of inductors decrease.

Figure 2(b) shows mode 2 equivalent circuit. During mode 2, the voltage across the inductors is:

$$V_{L1} + V_{L2} = V_{in} - V_{C2} = V_{in} - \frac{V_O}{2} \tag{6}$$

Duration of mode 2 is equal as:

$$t_2 = (\frac{1-D}{2}).T \tag{7}$$

Mode 3: T_1 is turned off and T_2 is turned on. In this mode D_3, D_{o1} are turned on and D_1, D_2 and D_{o2} are turned off. The energy is pumped to C_1 through T_2, and D_{o1}, so currents of inductor is decreased. Figure 2(c) shows mode

3 equivalent circuit. During mode 3, the voltage across the inductor is:

$$V_{L1} + V_{L2} = V_{in} - V_{C1} = V_{in} - \frac{V_O}{2} \qquad (8)$$

In this study value of L_1 is equal to L_2 so:

$$V_{L1} = V_{L2} \qquad (9)$$

$$i_{L1} = i_{L2} \qquad (10)$$

Duration of mode 3 is equal as:

$$t_3 = (\frac{1-D}{2}).T \qquad (11)$$

(a)

(b)

(c)
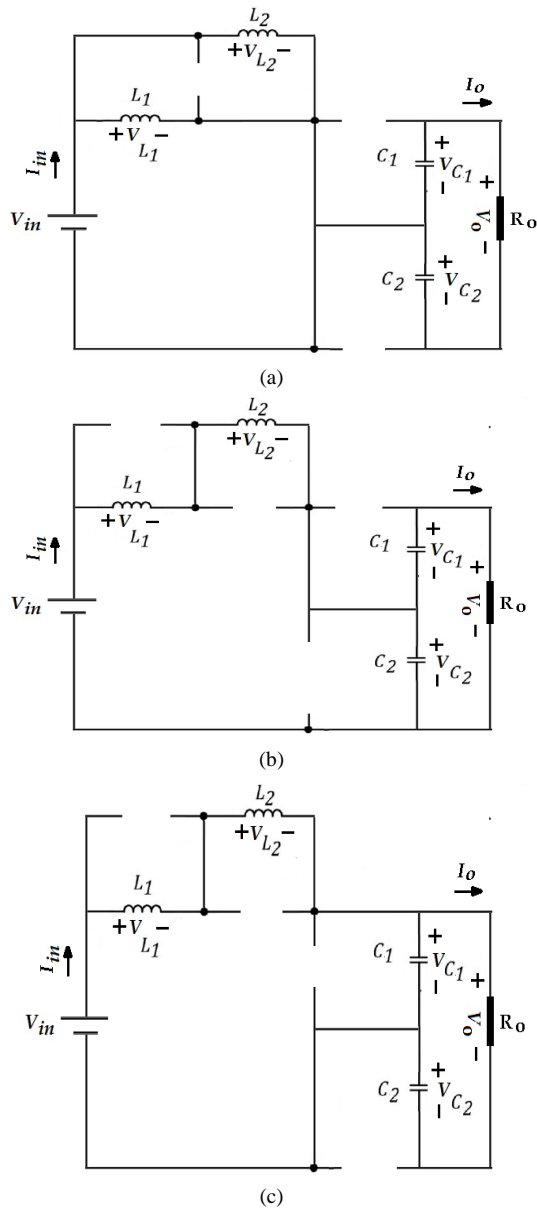
Fig. 2. Topological stages of the proposed converter (a) mode 1 (b) mode 2 and (c) mode 3.

The inductor average voltage over one cycle is zero [16].

$$\overline{V_{L1}} = 0 = D.V_{in} + \frac{2(1-D)}{2} \frac{(V_{in} - \frac{V_O}{2})}{2}$$

$$\Rightarrow V_O = \frac{2(1+D)V_{in}}{(1-D)} \qquad (12)$$

Figure 3 shows the voltage gain for different duty ratio.
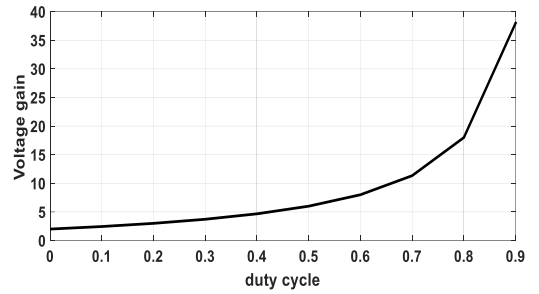
Fig. 3. Voltage gain for different duty ratio.

The current of capacitor is:

$$i_{C1} = \begin{cases} -I_O & DT \\ (I_{L1} - I_O) & \frac{(1-D)}{2} \\ -I_O & \frac{(1-D)}{2} \end{cases} \qquad (13)$$

The capacitor average current over one cycle is zero [16].

$$\overline{i_{c1}} = 0 \Rightarrow$$

$$-D.I_O + \frac{(1-D)}{2}(I_{L1} - I_O) - \frac{(1-D)}{2}I_O = 0$$

$$I_{L1} = I_{L2} = \frac{2I_O}{(1-D)} \qquad (14)$$

If C_1 is equal to C_2 then the voltage ripple of output capacitors are shown as:

$$\Delta V_{C1} = \Delta V_{C2} = \frac{(1+D)}{2fC_1}I_O \qquad (15)$$

The root mean square current of capacitors can be calculated as follows

$$I_{C1} = I_{C2} = \sqrt{\frac{(1+D)}{(1-D)}}I_O \qquad (16)$$

Figure 4 shows the signal gates and voltage of semiconductors, inductors and capacitors. The charge

and discharge of L_2 is the same as L_1. The frequency of inductor voltage is double of switching frequency.
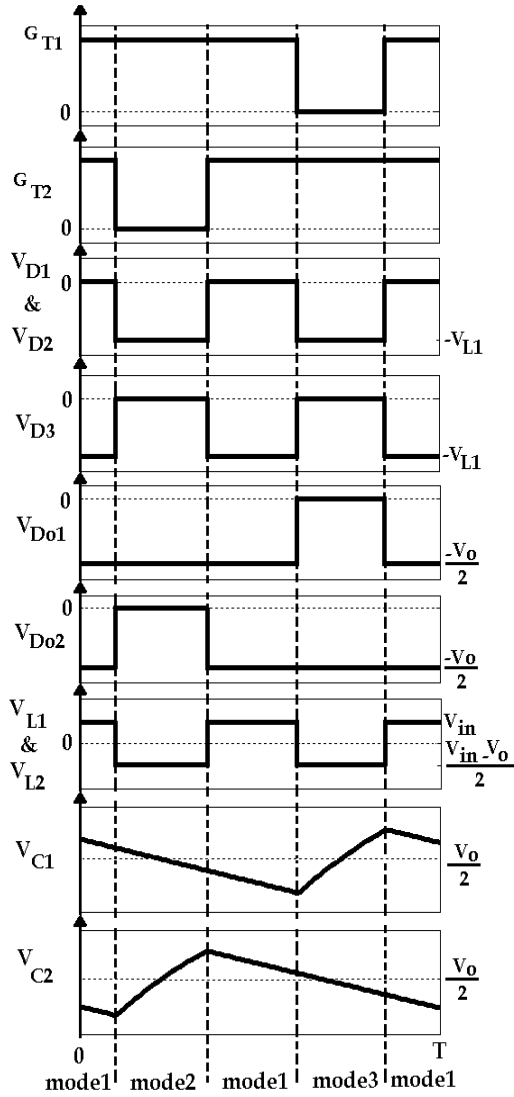
Fig. 4. The signal gates and voltage of components.

Based on Eq. (12), the input current I_{in} can be expressed as:

$$I_{in} = \frac{2(1+D)I_O}{(1-D)} \qquad (17)$$

Where, I_O is the output current. In addition, the current ripple of i_{L1} and i_{L2} denoted by Δi_{L1} and Δi_{L2}, respectively. The current ripple of inductors can be expressed to be

$$\Delta i_{L1} = \Delta i_{L2} = \frac{D.T}{2L_1} V_{in} \qquad (18)$$

$$\Delta i_{in} = I_{L1} + 3\Delta i_{L1} = \frac{2I_O}{(1-D)} + \frac{3D.T}{4L_1} V_{in} \qquad (19)$$

The ripple of inductor current is half of ripple of inductor current in classic boost DC/DC converter. This is one advantage of three-level converters [10-12].

Figure 5 shows voltage and current of one inductor in DCM condition. By equating the average value of this v_L waveform to zero, one obtains:

$$\overline{V_{L1}} = 0 = D_1 V_{in} + D_2 \frac{(V_{in} - V_O)}{2} \Rightarrow$$

$$D_2 = \frac{2D_1 V_{in}}{(V_O - V_{in})} \qquad (20)$$

The dc component of the D_{o1}, $\overline{i_{Do1}}$, is:

$$\overline{i_{Do1}} = \frac{K_1 K_2 V_{in} T}{2L_1} = I_o = \frac{V_o}{R} \qquad (21)$$

By inserting Eq. (20) into Eq. (21), and rearranging terms, one obtains the following quadratic equation:

$$\frac{TK_1^2 V_{in}^2}{L_1(V_O - V_{in})} = \frac{V_o}{R}$$

$$V_o^2 - V_{in} V_o - \frac{RK_1^2 V_{in}^2 T}{L_1} = 0 \qquad (22)$$

Suppose that τ is defined as:

$$\frac{L_1}{RT} = \tau \qquad (23)$$
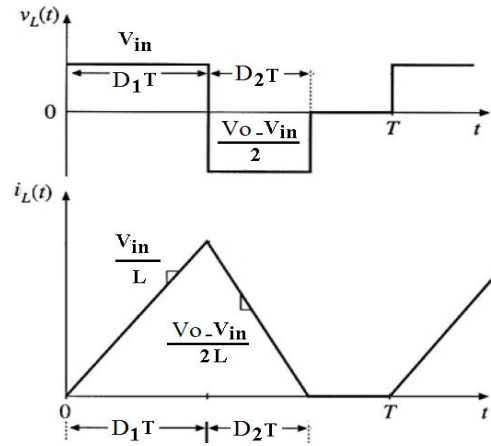
Fig. 5. Voltage and current of one inductor.

Then, the voltage boosting gain of the proposed converter in DCM condition is found as

$$\frac{V_o}{V_{in}} = \frac{1 \pm \sqrt{1 + \frac{4K_1^2}{\tau}}}{2} \qquad (24)$$

2.2. Voltage ratings of semiconductors

An important problem in power electronic converters is the ratings of semiconductors. In other word, voltage and current ratings of the semiconductors in a converter play important roles on the cost and realization. The voltage stresses on semiconductor are given as:

$$V_{T1} = V_{T2} = V_{Do1} = V_{Do2} = \frac{V_O}{2} = \frac{(1+D)V_{in}}{(1-D)} \quad (15)$$

$$V_{D1} = V_{D2} = \frac{DV_{in}}{(1-D)} \quad (26)$$

$$V_{D3} = V_{in} \quad (37)$$

2.3. Power loss calculation

Generally, power electronic converters have losses. Different elements in proposed converter such as inductors, capacitors and semiconductor generate power loss [17]. Fig. 6 shows an equivalent circuit of the proposed converter with parasitic resistances.

The passive components, capacitors and inductors have internal resistant. The conduction losses of inductors L_1 and L_2 are

$$P_{RL1} = R_{L1}I_{L1}^2 = \frac{4R_{L1}I_O^2}{(1-D)^2} \quad (48)$$

$$P_{RL2} = R_{L2}I_{L2}^2 = \frac{4R_{L2}I_O^2}{(1-D)^2} \quad (59)$$
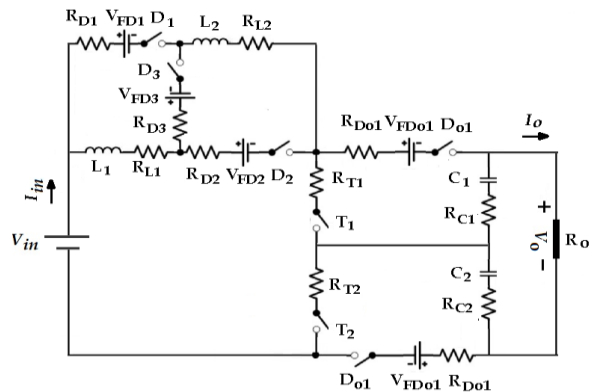
Fig. 6. Equivalent circuit of the proposed converter with parasitic resistances.

The power losses in capacitors C_1 and C_2 are

$$P_{RC1} = R_{C1}I_{C1}^2 = \frac{R_{C1}(1+D)I_O^2}{(1-D)} \quad (30)$$

$$P_{RC2} = R_{C2}I_{C2}^2 = \frac{R_{C2}(1+D)I_O^2}{(1-D)} \quad (31)$$

The conduction losses of the diodes can be calculated as

$$P_{RD1} = P_{RD2} = R_{D1}I_{D1}^2 = \frac{4R_{D1}DI_O^2}{(1-D)^2} \quad (32)$$

$$P_{VD1} = P_{VD2} = V_{FD1}I_{D1ave} = \frac{2DV_{FD1}I_O}{(1-D)} \quad (33)$$

$$P_{RDo1} = P_{RDo2} = R_{Do1}I_{Do1}^2 = \frac{2R_{Do1}I_O^2}{(1-D)} \quad (34)$$

$$P_{VDo1} = P_{VDo2} = V_{FDo1}I_{Do1ave} = V_{FDo1}I_O \quad (35)$$

$$P_{RD3} = R_{D3}I_{D3}^2 = \frac{4R_{D3}I_O^2}{(1-D)} \quad (36)$$

$$P_{VD3} = V_{FD3}I_{D3ave} = V_{FD3}I_O \quad (37)$$

Where R_D and V_{FD} are the diode resistance and threshold voltage.

The conduction loss of the power switch is

$$P_{RT1} = P_{RT2} = R_{T1}I_{T1}^2 = \frac{2(7D+1)R_TI_O^2}{(1-D)^2} \quad (38)$$

Where R_T is switch on-resistance. The switching losses are due to non-ideal operation of switches [20].

$$P_{swT1} = P_{swT2} = (E_{on} + E_{off})f \quad (39)$$

Where E_{on} and E_{off} are turn on and off energy losses in switch.

2.4. Extended topology

The proposed topology gives high transfer ratio. To obtain bigger gain, switched inductor circuits can be added to main structure as shown in Fig. 7.

In this state, the voltage gain is deduced in the following equation

$$V_O = \frac{2(1+nD)V_{in}}{(1-D)} \quad (40)$$

Where n is the number of switched inductor cells.

3. COMPARISION STUDY

Figure 8 shows cascaded boost converter. For comparison study between cascaded boost converter and presented topology, Tables 1 is presented.
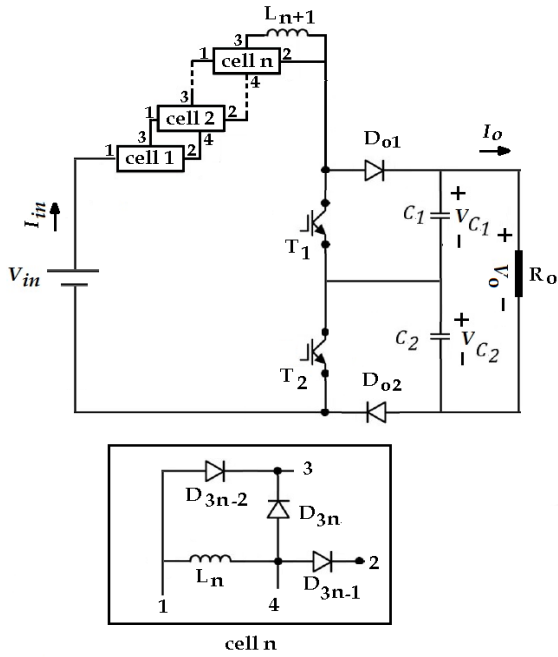
Fig. 7. Presented topology with additional switched inductor cells.

Table 1. comparison between the proposed converter and cascaded boost converter

Presented	Cascaded boost
$\dfrac{V_O}{V_{in}} = \dfrac{2(1+D)}{(1-D)}$	$\dfrac{V_O}{V_{in}} = \dfrac{1}{(1-D)^2}$
Sum of voltage stress of semiconductor	
$\dfrac{(5+4D)}{2(1+D)}V_O$	$(4-2D)V_O$
voltage stress of semiconductor	
$V_{T1} = V_{T2} = \dfrac{V_O}{2}$ $V_{D1} = V_{D2} = \dfrac{DV_O}{2(1+D)}$ $V_{Do1} = V_{Do2} = \dfrac{V_O}{2}$	$V_{T1} = V_{D2} = (1-D)V_O$ $V_{T3} = V_{D4} = V_O$
Capacitor voltage	
$V_{C1} = V_{C2} = \dfrac{V_O}{2}$	$V_{Co} = V_O$ $V_{C1} = (1-D)V_O$

As can be seen in Tables 1, comparison has been performed between the proposed converter and conventional cascaded boost converter in ideal case. It is obvious that the gain of the proposed converter is higher than the conventional boost converter and cascaded boost converter. The number of components in presented topology is higher than cascaded converter while the voltage stress of elements is lower than cascaded converter. The cost of semiconductor has direct relation to voltage stress.

3.   Experimental Results

A switched inductor three-level converter using a one switched inductor circuit was built in the laboratory.
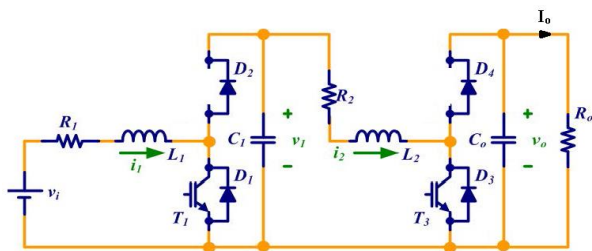
Fig. 8. Cascaded boost topology.

The simulation and experimental results show operation of presented converter. Figure 9 shows circuit of DC/DC converter. The values used in the prototype are shown in Table 2. The output voltage is 137 V.

The nominal load is 400 Ω, which results in an output current of 0.34 A, and an output power of 47W. The selected operating switching frequency is 15800 Hz. Fig. 10 shows gate pulse of DC/DC converter. In any time one or two switch is on. The voltage and current of L_1 is shown in Fig. 11.
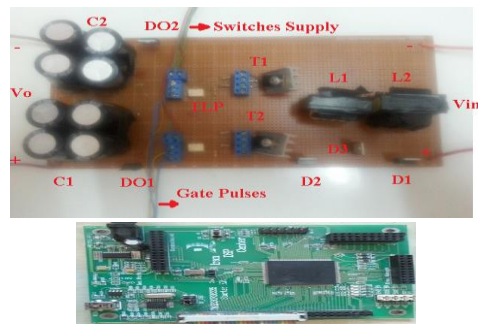
Fig. 9. Circuit of DC/DC converter.

Table 2. Parameters

DC source	24 V
L_1, L_2	500μH
C_1, C_2	1000 μF
Switching frequency	15800 Hz
R	400 ohm
D	0.5
MOSFET driver	TLP250
MOSFET	IRFP460
Diode	U1560
Controller	DSPTMS320F28335
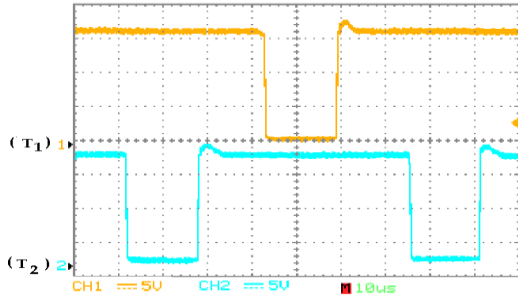
Fig. 10. Gate pulses of DC/DC converter.

(a)
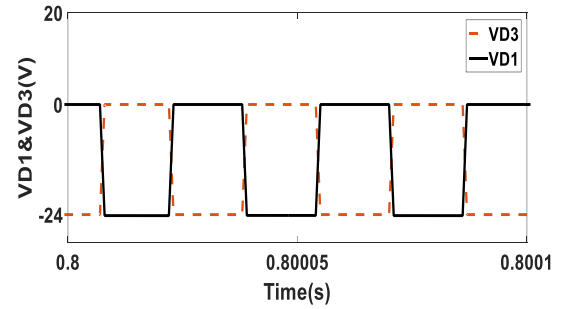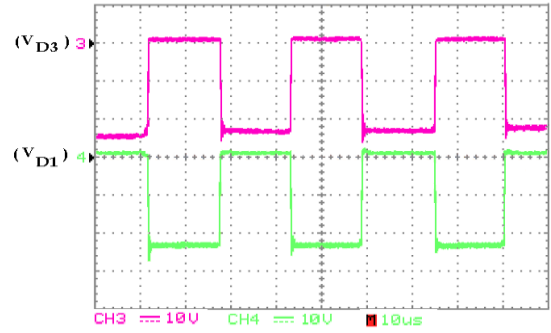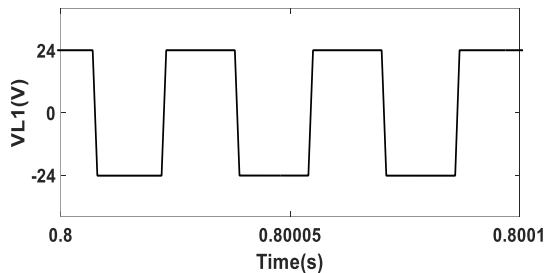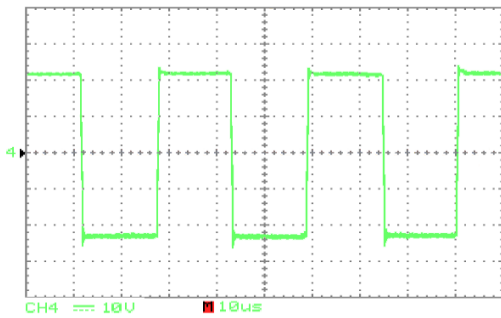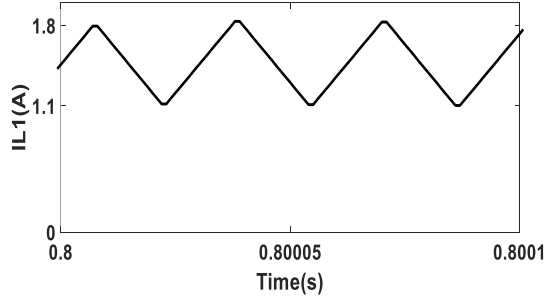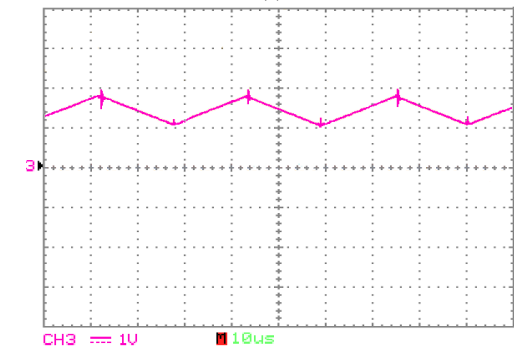
Fig. 11. Voltage and Current of L_1 (a) voltage and (b) current.

(b)
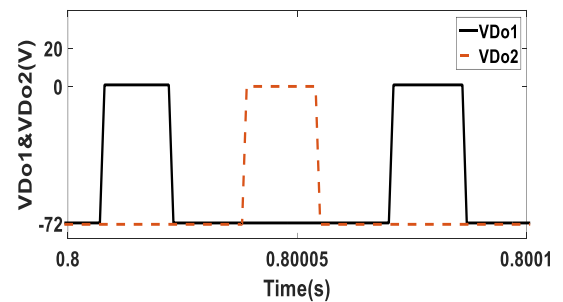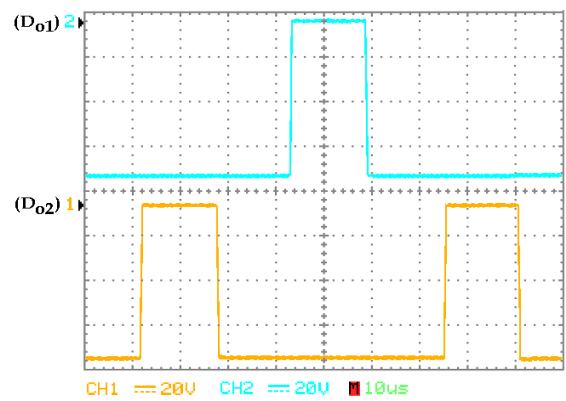
Fig. 12. Voltage of D_1 and D_3.

The voltage of L_2 is the same as L_1. Figure 12 shows voltage of D_1 and D_3. The voltage of D_2 is the same as D_1. The turning on and off of D_1 and D_2 is reverse of D_3.

In Fig. 12 channel 3 shows voltage of D_3 and channel 4 shows voltage of D_1. The voltage of output diodes (D_{o1} and D_{o2}) are shown in Fig. 13. It is clear that both output diodes don't on simultaneously. Figure 14 shows input current and output voltage of DC/DC converter.

Fig. 13. Voltage of output diodes.

REFERENCES

[1] S. M. Alizadeh Shabestary, M. Saeedmanesh, A. Rahimi Kian, and E. Jalalabadi, "Real-time frequency and voltage control of an islanded mode microgrid," *J. Iran. Assoc. Electr. Electron. Eng.*, vol. 12, no. 3, pp. 9-14, 2015.

[2] E. Salary, M. R. Banaei, A. Ajami, "Design of novel step-up boost dc/dc converter, "*Iran. J. Sci. Technol. Trans. Electr. Eng.*, vol. 41pp.13-22, 2017.

[3] E. Salary, M. R. Banaei, A. Ajami, "Step-up DC/DC converter based on partial power processing, "*Gazi Univ. J. Sci.,* vol. 28, no. 4, pp.599-607, 2015.

[4] E. Salary, M. R. Banaei, A. Ajami, "Multi-stage DC-AC converter based on new DC-DC converter for energy conversion," *J. Oper. Autom. Power Eng.*, vol. 4, pp. 42-53, 2016.

[5] A. Asghar Ghadimi, H. Rastegar, and A. Keyhani, "Development of average model for control of a full bridge PWM DC-DC converter," *J. Iran. Assoc. Electr. Electron. Eng.*, vol. 4, no. 2, pp. 52-59, 2007.

[6] W. Li, and X. He, "Review of nonisolated high-step-up dc/dc converters in photovoltaic grid-connected applications," *IEEE Trans. Ind. Electron.*, vol. 58, no. 4, pp. 1239-1250, 2011.

[7] K. Shu-Kong, and D. D. C.Lu, "A high step-down transformerless single-stage single-switch AC/DC converter," *IEEE Trans. Power Electron.*, vol. 28, no. 4, pp. 36-45, 2013.

[8] E. H. Ismail, M. A. Al-Saffar, and A. J. Sabzali, "High conversion ratio DC–DC converters with reduced switch stress," *IEEE Trans. Circuits Syst. I*, vol. 55, no. 7, pp. 2139- 2151, 2008.

[9] Y. Jang, and M. M. Jovanovic, "Interleaved boost converter with intrinsic voltage-doubler characteristic for universal-line PFC front end", *IEEE Trans. Power Electron.*, vol. 22, no. 4, pp. 1394 - 1401, 2007.

[10] F. S. Garcia, J. A. Pomilio, and G. Spiazzi, "Modeling and control design of the six-phase interleaved double dual boost", *Proc. 9ᵗʰ IEEE Int. Conf. Ind. Appl.* , 2010, pp. 1-6.

[11] S. Choi, V. G. Agelidis, J. Yang, D. Coutellier, and P. Marabeas, "Analysis, design and experimental results of a floating-output interleaved-input boost-derived dc–dc high-gain transformer-less converter," *IET Power Electron.,* vol. 4, no. 1, pp. 168-180, 2011.

[12] F. S. Garcia, J. A. Pomilio, and G. Spiazzi, "Modeling and control design of the interleaved double dual boost converter," *IEEE Trans. Ind. Electron.*, vol. 60, no. 8, pp. 3283-3290, 2013.

[13] H. Nomura, K. Fujiwara, and M. Yoshida, "A new DC-DC converter circuit with larger step-up/down ratio," *Proc. 37ᵗʰ IEEE Power Electron. Spec. Conf.,* pp.1 - 7, 2006.

[14] Y. Zhang, and and J. Liu, "Improved pulse-width modulation of diode-assisted buck-boost voltage source inverter," *IEEE Trans. Power Electron.*, vol. 28, no. 8, pp. 3675-3699, 2013.

[15] K.I. Hwu, and W.Z. Jiang, "Voltage gain enhancement for a step-up converter constructed by KY and buck-boost converters," *IEEE Trans. Ind. Electron.*, vol. 61, no. 4, pp. 1758-1768, 2014.

[16] M. R. Banaei, H. Ardi, and A. Farakhor, "Analysis and implementation of a new single-switch buck–boost DC/DC converter," *IET Power Electron.*, vol. 7, no. 7, pp.1906-1914, 2014.

Fig. 14. Two main waveforms of DC/DC converter (a) input current and (b) output voltage.

4. CONCLUSIONS

A new configuration of boost DC/DC converter has been proposed. The proposed converter is a boost converter that has a higher gain than the conventional boost converter. The suggested topology needs switches and diodes with low standing voltage on semiconductors. Analyses have been provided to validate the proposed system idea. The operation and performance of the proposed converter has been verified on a prototype.

[17] M. El-Sayed Ahmed, and M. Orabi, O. M. AbdelRahim, "Two-stage micro-grid inverter with high-voltage gain for photovoltaic applications," *IET Power Electron*., vol. 6, no. 9, pp. 1812-1821, 2013.

[18] V. Yaramasu, B. Wu, M. Rivera, and J. Rodriguez, "A new power conversion system for megawatt PMSG wind turbines using four-level converters and a simple control scheme based on two-step model predictive strategy—part i: modeling and theoretical analysis," *IEEE J. Emerging Sel. Top. Power Electron.*, vol. 2, no. 1, pp. 3-13, 2014.

[19] S. Krithiga, and N. Ammasai Gounden, "Investigations of an improved PV system topology using multilevel boost converter and line commutated inverter with solutions to grid issues," *Simul. Modell. Pract. Theory*, 2014, 42, pp. 147-159.

[20] M. F. Kangarlu, and E. Babaei, "A generalized cascaded multilevel inverter using series connection of submultilevel inverters," *IEEE Trans. Power Electron.*, vol. 28, no. 2, pp. 625-636, Feb. 2013.

[21] M. R. Banaei, E. Salary, "Application of multi-stage converter in distributed generation systems," *Energy Convers. Manage.*, vol. 62, pp. 76-83, 2012.